

Cell Reports, Volume 42

## Supplemental information

**Molecular basis for differential activation**

**of p101 and p84 complexes**

**of PI3K $\gamma$  by Ras and GPCRs**

**Manoj K. Rathinaswamy, Meredith L. Jenkins, Benjamin R. Duewell, Xuxiao Zhang, Noah J. Harris, John T. Evans, Jordan T.B. Stariha, Udit Dalwadi, Kaelin D. Fleming, Harish Ranga-Prasad, Calvin K. Yip, Roger L. Williams, Scott D. Hansen, and John E. Burke**

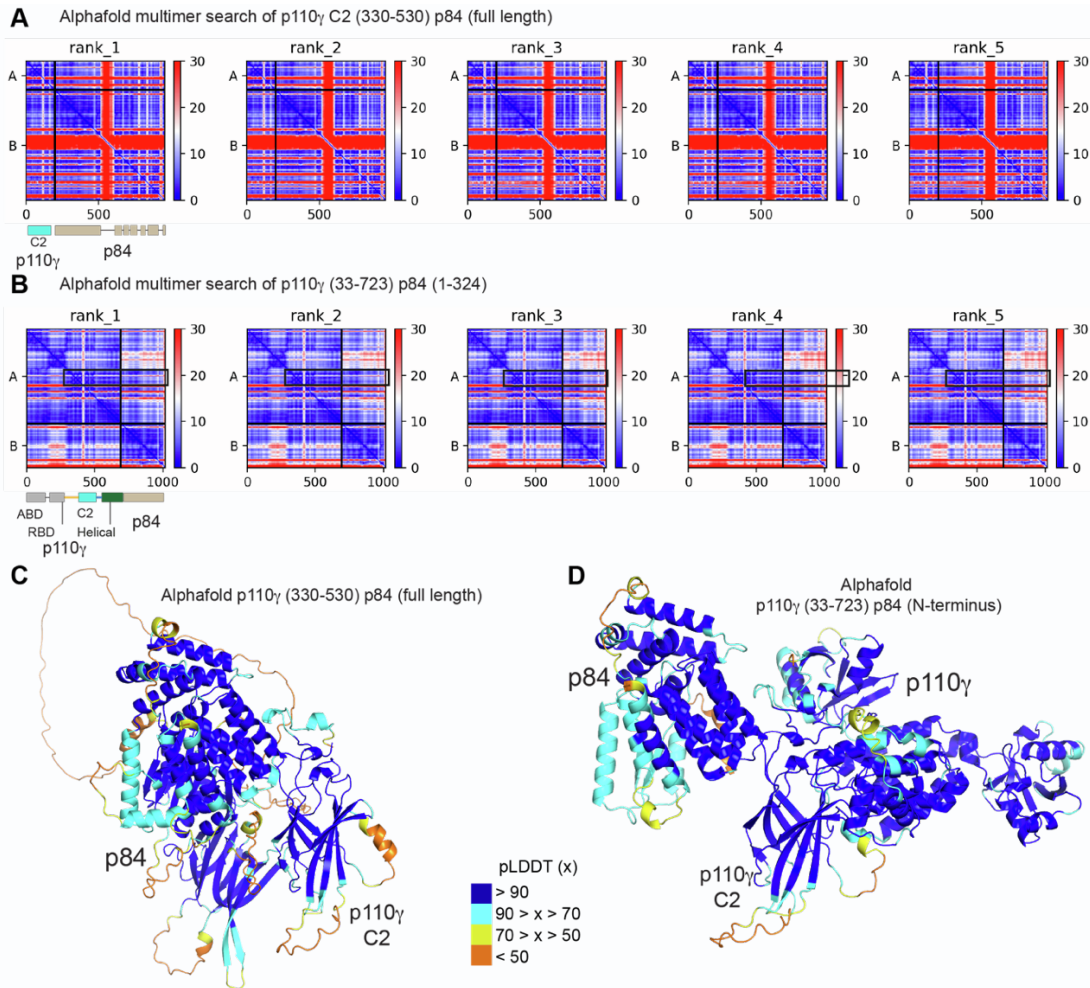


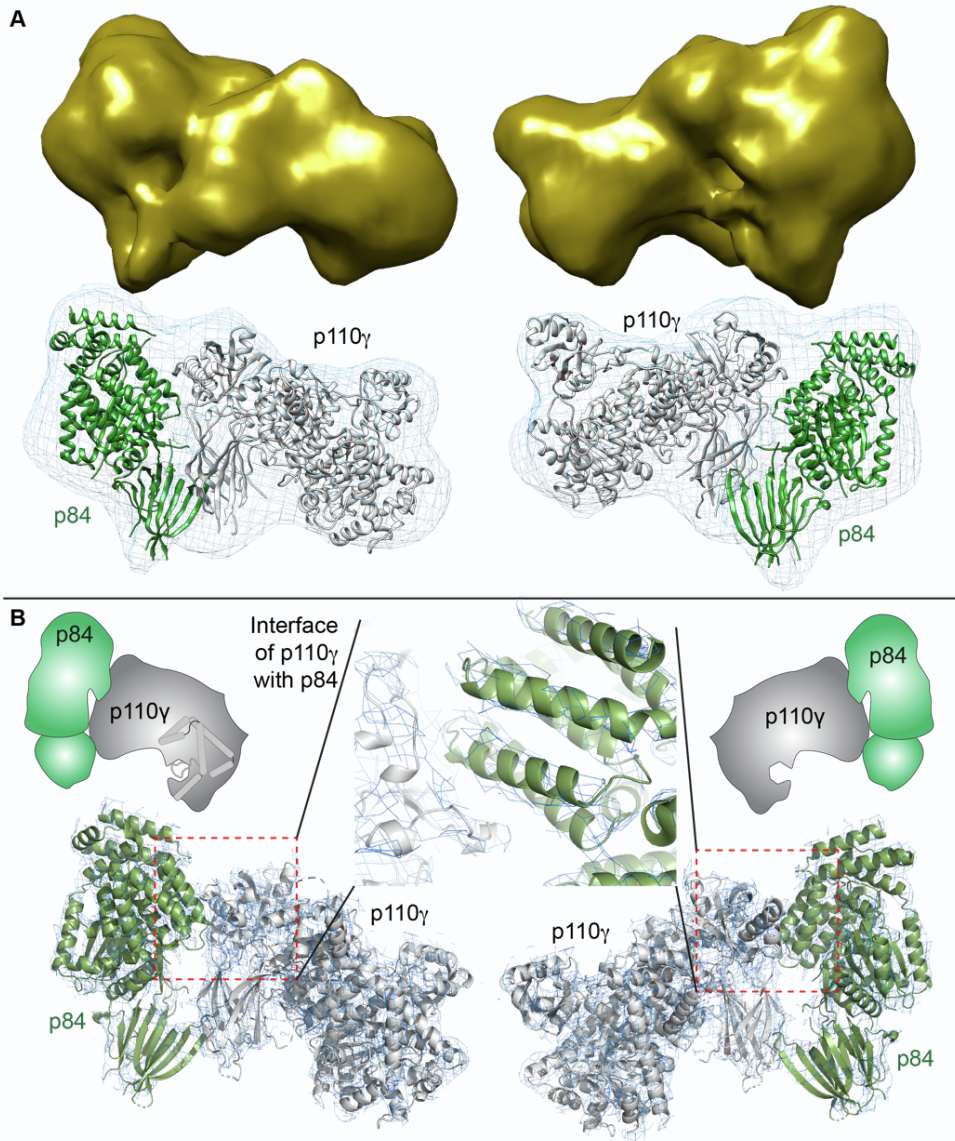
**Fig S1. AlphaFold2-multimer modelling of the p110 $\gamma$ -p84 complex (related to Fig 1).**

**A.** Predicted aligned error (PAE) for AlphaFold2 Multimer search of the p110 $\gamma$  C2 domain and RBD-C2 and C2-helical linkers bound to full length p84. The sequence of the two searches are indicated, with a schematic indicated below.

**B.** Predicted aligned error (PAE) for AlphaFold2 Multimer search of the N-terminus of p110 $\gamma$  (33-723 covering the ABD, RBD, C2, and helical domains) and the N-terminus (1-324) of p84. The sequence of the two searches are indicated, with a schematic indicated below. For both panels **A+B**, the colours indicate the predicted aligned error, and are coloured according to the legend. Note that the PAE plot is not an inter-residue distance map or a contact map. Instead, the red-blue colour indicates expected distance error. The colour at (x, y) corresponds to the expected distance error in residue x's position, when the prediction are aligned on residue y (more information can be found at <https://alphafold.ebi.ac.uk/>)<sup>1,2</sup>. Blue is indicative of low PAE, with the low PAE at the p110 $\gamma$ -p84 interface in both panels **A+B** suggests that AlphaFold2-multimer predicts the relative positions of the catalytic and regulatory subunits with high accuracy.

**C+D.** AlphaFold2 models from panels **A+B** shown with the per-residue confidence metric predicted local-distance difference test (pLDDT) coloured according to the legend. The pLDDT score varies from 0 to 100,

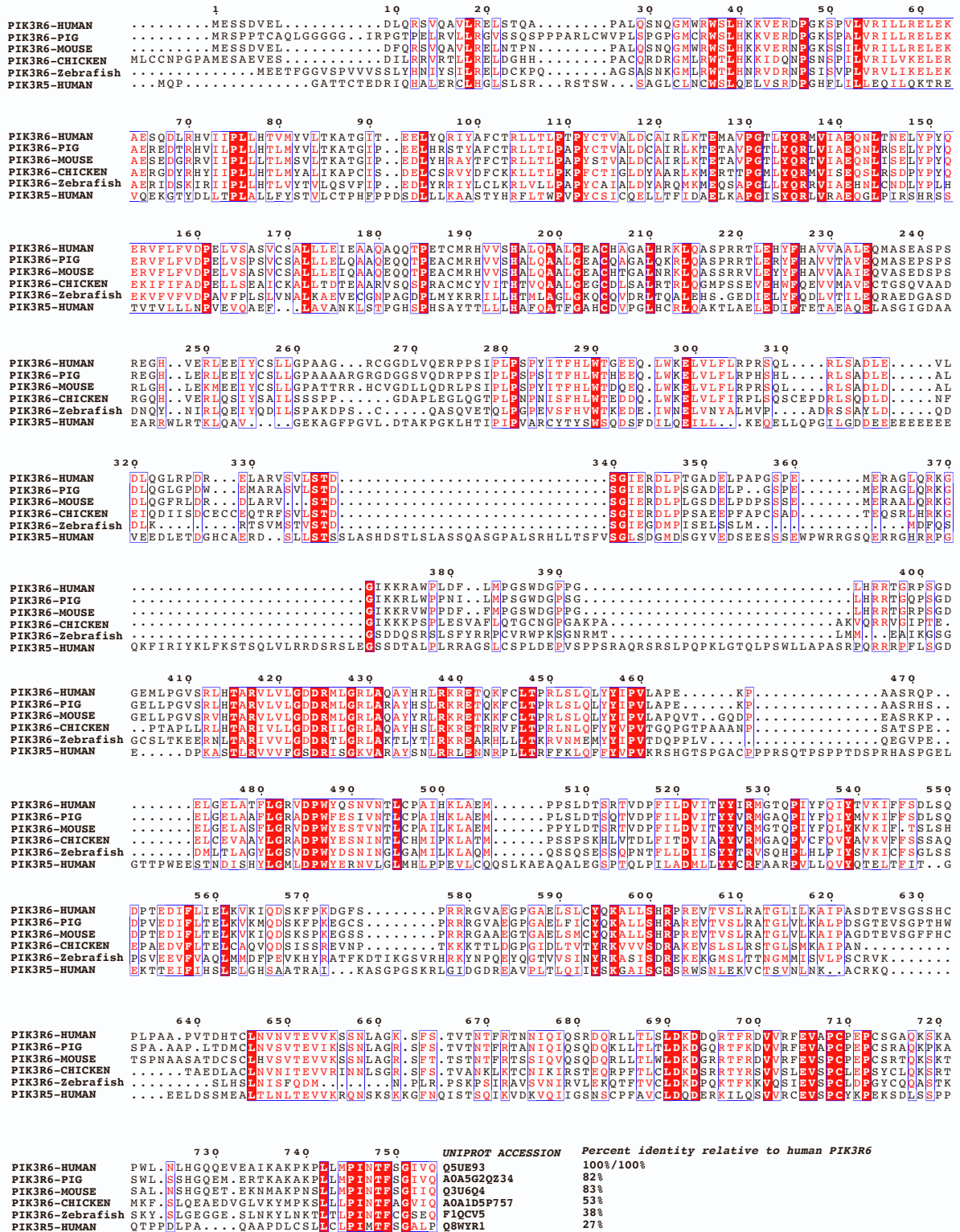
17 and is an estimate of how well the prediction would agree with an experimental structure based on the local  
18 distance difference test  $C\alpha$  <sup>1</sup>.  
19



20  
21 **Fig S2. EM and X-ray validation of the alphafold2-multimer model of the p110 $\gamma$ -p84 complex (related**  
22 **to Fig 1).**

23 **A.** 3D EM reconstruction of p110 $\gamma$  with different orientations of the complex. A cartoon representation of  
24 the p110 $\gamma$ -p84 complex is shown in the density map in the same orientation as above.

25 **B.** The 2mFo-DFc electron density (contoured at 1.5 $\sigma$ ) for the complex of the porcine p110 $\gamma$  and mouse  
26 p84 complex phased using the alphafold2 generated model. A zoom in of the interface of the p110 $\gamma$ -p84  
27 complex shows clear density across for the interfacial helices in p84 (green).



28

29

**Fig S3. Alignment of p84 orthologs (PIK3R6), and comparison to p101 (PIK3R5) (related to Fig 2)**

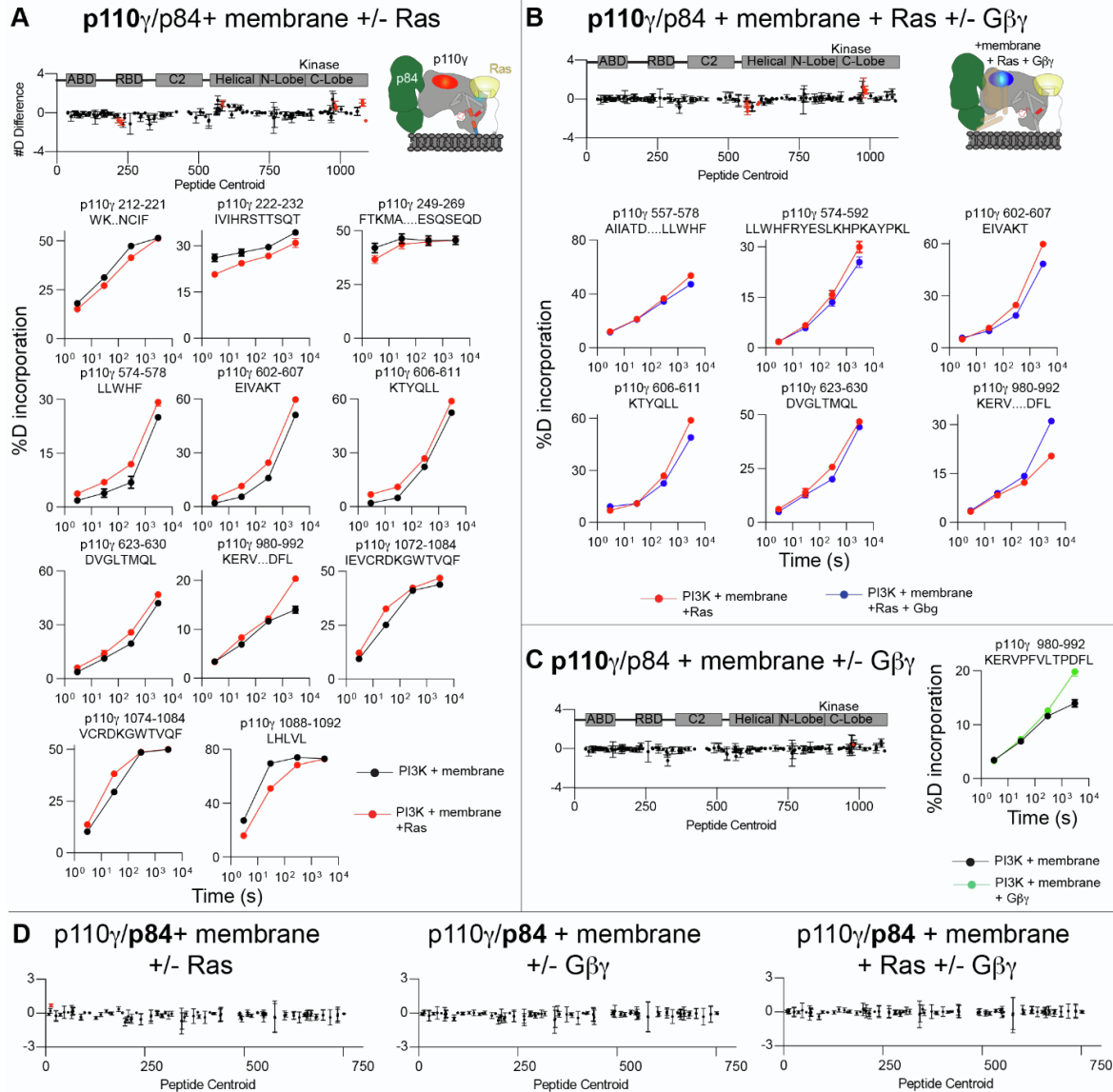
30

The alignment for the indicated genes is shown, with the UNIPROT accession numbers shown in the bottom

31

right, along with the percent identity compared to human PIK3R6.





32

33

34

35

36

37

38

39

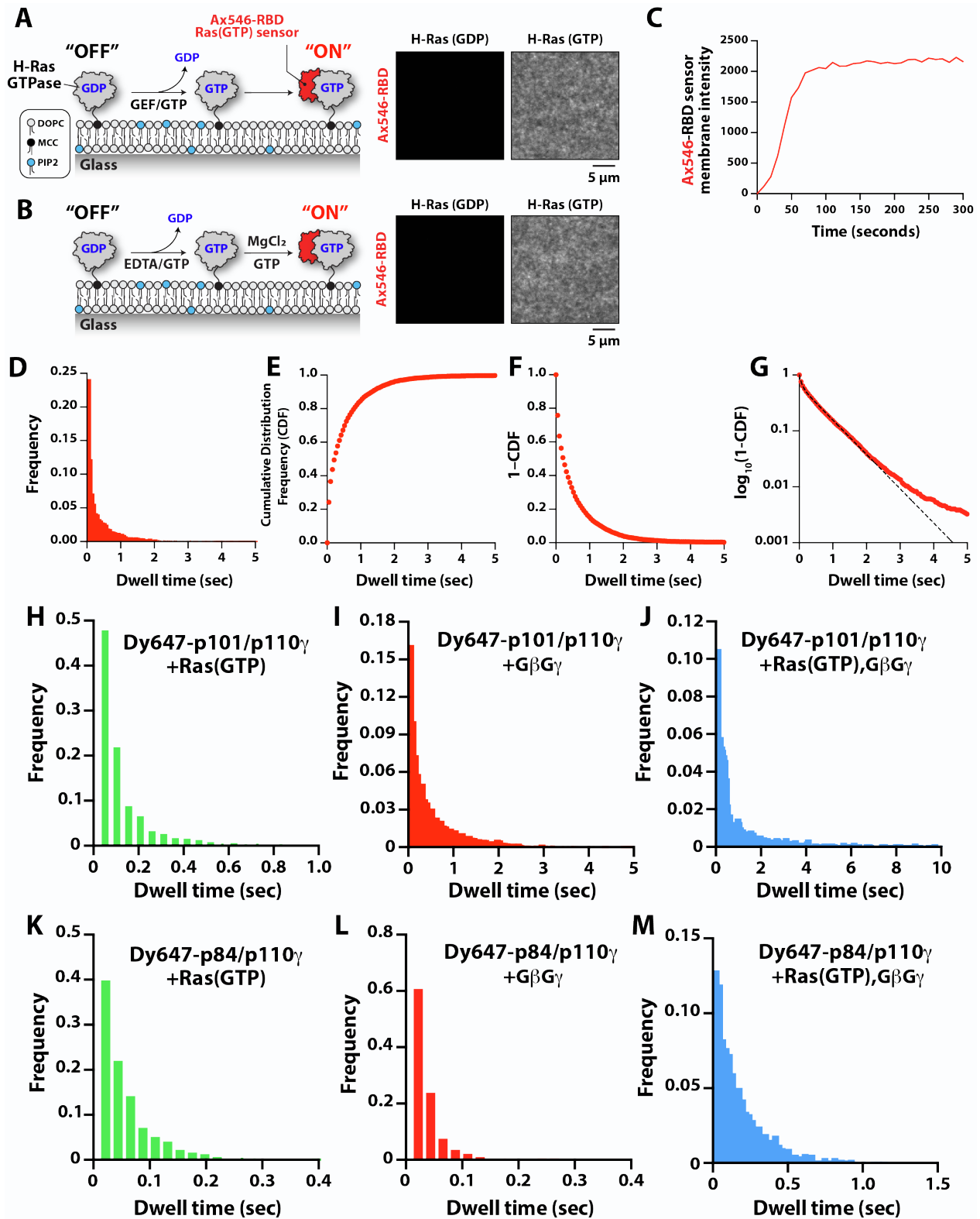
40

41

42

43

**Fig S4. Raw HDX-MS data (A-D) (related to Fig 4).** The sum of the number of deuterium differences in the p110 $\gamma$  subunit between plasma membrane mimic vesicles and (A) plasma membrane mimic vesicles with 3  $\mu$ M GTP $\gamma$ S loaded lipidated Hras and (B) plasma membrane mimic vesicles with 3  $\mu$ M GTP $\gamma$ S loaded lipidated Hras 3  $\mu$ M G $\beta\gamma$  and (C) plasma membrane mimic vesicles with 3  $\mu$ M G $\beta\gamma$ . The sum of the number of deuterium differences in the p84 subunit under all conditions is shown in panel D. Each point is representative of the centre residue of an individual peptide. For all number of deuterium difference graphs the peptides that met the significance criteria are coloured red. Error is shown in the #D difference graphs as the sum of the standard deviation across all time points (n=3 for each time point). Selected deuterium exchange incorporation curves for peptides in the presence and absence of HRas and or G $\beta\gamma$  are shown below and are coloured according to the legend. Error in the %D peptide incorporation graphs is shown as standard deviation (n=3), with most error bars smaller than the size of the point.

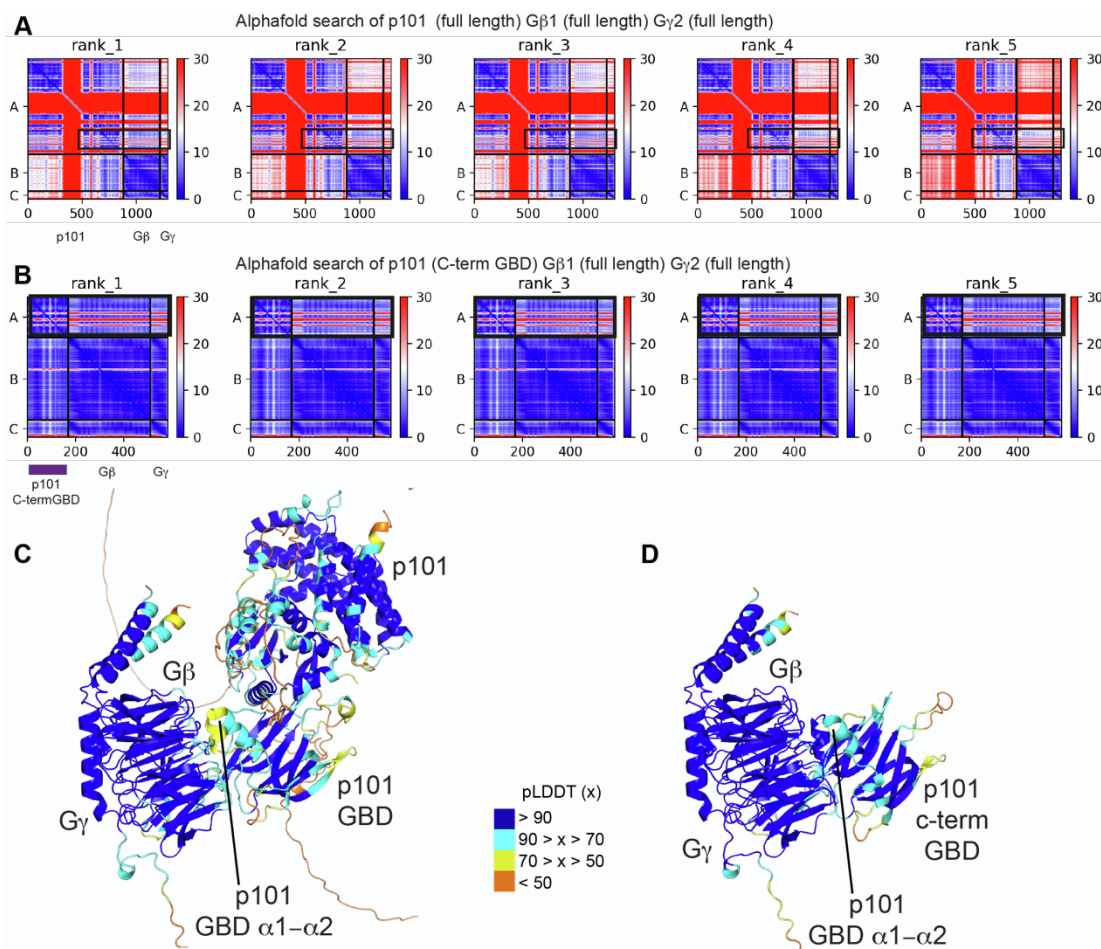


44

45 Fig S5. Validation of H-Ras supported membrane conjugation and activation and single molecule

46 TIRF-M dwell time distribution plots (related to Fig 5)

47 **A.** Scheme for activating membrane conjugated H-Ras with a guanine nucleotide exchange factor (GEF).  
48 Representative images showing the membrane localization of 50 nM Alexa546-SNAP-RBD visualized in  
49 the absence (left) or presence (right) of 50 nM SosCat. For all data in this figure the data shown is  
50 representative data, with full kinetic parameters shown in Table S3 generated from 2-4 technical replicates.  
51 **B.** Scheme for activating membrane conjugated H-Ras using EDTA-based nucleotide exchange of GDP  
52 for GTP. Representative images showing the membrane localization of 50 nM Alexa546-SNAP-RBD  
53 visualized before and after chemical activation of H-Ras.  
54 **C.** Kinetics of H-Ras activation measured in the presence of 50 nM SosCat (GEF) and 50 nM Alexa546-  
55 SNAP-RBD. Membrane composition for panels **A-C** was: 96% DOPC, 2% PI(4,5)P<sub>2</sub>, 2% MCC-PE. Images  
56 acquired using TIRF-M.  
57 **D-G.** Representative single molecule dwell distributions based on data collected in the presence of 10 pM  
58 DY647-p101-p110γ on SLBs containing Gβγ. Plot demonstrate workflow for generating single molecule  
59 dwell time distribution plots showing in Figure 5E-5F. **(D)** Frequency distribution plot. **(E)** Cumulative  
60 distribution frequency plot. **(F)** Inverse plot of cumulative distribution frequency plot (i.e. 1-CDF). **(G)** 1-CDF  
61 curve plotted on a log scale.  
62 **H-M.** Representative frequency distribution plots for the data sets plotted in Figure 5E-5F. Membrane  
63 composition for panels **H-M** was: 96% DOPC, 2% PI(4,5)P<sub>2</sub>, 2% MCC-PE. Data collected by smTIRF-M.  
64  
65  
66



67

68 **Fig S6. AlphaFold2 multimer modelling of the complex between p101 and Gβγ (related to Fig 6)**

69 **A.** Predicted aligned error (PAE) for AlphaFold2 Multimer search of full length p101, Gβ1, and Gγ2. The  
 70 sequence of the two searches are indicated.

71 **B.** Predicted aligned error (PAE) for AlphaFold2 Multimer search of the C-terminus of p101, Gβ1, and Gγ2.

72 The sequence of the two searches are indicated, with a schematic indicated below. For both panels A+B,

73 the colours indicate the predicted aligned error, and are coloured according to the legend. Note that the

74 PAE plot is not an inter-residue distance map or a contact map. Instead, the red-blue colour

75 indicates expected distance error. The colour at (x, y) corresponds to the expected distance error in residue

76 x's position, when the prediction are aligned on residue y (more information can be found at

77 <https://alphafold.ebi.ac.uk/>)<sup>1,2</sup>. Blue is indicative of low PAE, with the low PAE at the p101-Gβγ interface in

78 both panels A+B suggests that AlphaFold2-multimer predicts the relative positions with high accuracy.

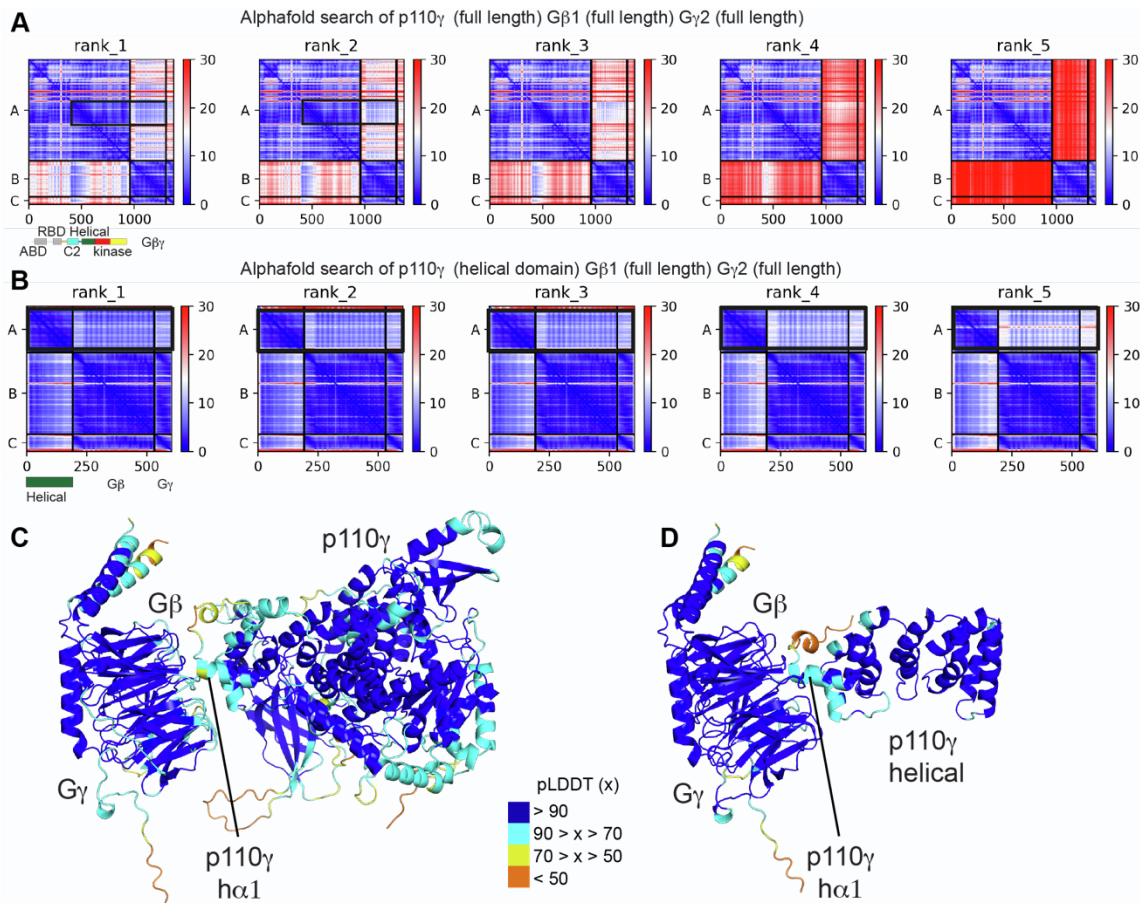
79 **C+D.** AlphaFold2 models from panels **A+B** shown with the per-residue confidence metric predicted local-

80 distance difference test (pLDDT) coloured according to the legend. The pLDDT score varies from 0 to 100,

81 and is an estimate of how well the prediction would agree with an experimental structure based on the local

82 distance difference test Ca<sup>1</sup>.





83

84 **Fig S7. AlphaFold2 multimer modelling of the complex between p110 $\gamma$  and G $\beta\gamma$  (related to Fig 6)**

85 **A.** Predicted aligned error (PAE) for AlphaFold2 Multimer search of full length p110 $\gamma$ , G $\beta$ 1, and G $\gamma$ 2. The  
 86 sequence of the two searches are indicated, with a schematic indicated below.

87 **B.** Predicted aligned error (PAE) for AlphaFold2 Multimer search of the helical domain of p110 $\gamma$ , and full  
 88 length G $\beta$ 1, and G $\gamma$ 2. The sequence of the two searches are indicated, with a schematic indicated below.

89 For both panels A+B, the colours indicate the predicted aligned error, and are coloured according to the  
 90 legend. Note that the PAE plot is not an inter-residue distance map or a contact map. Instead, the red-blue  
 91 colour indicates expected distance error. The colour at (x, y) corresponds to the expected distance error in  
 92 residue x's position, when the prediction are aligned on residue y (more information can be found at  
 93 <https://alphafold.ebi.ac.uk/>)<sup>1,2</sup>. Blue is indicative of low PAE, with the low PAE at the helical domain-G $\beta\gamma$   
 94 interface in both panels A+B suggests that AlphaFold2-multimer predicts the relative positions with high  
 95 accuracy.

96 **C+D.** AlphaFold2 models from panels **A+B** shown with the per-residue confidence metric predicted local-  
 97 distance difference test (pLDDT) coloured according to the legend. The pLDDT score varies from 0 to 100,  
 98 and is an estimate of how well the prediction would agree with an experimental structure based on the local  
 99 distance difference test Ca<sup>1</sup>.

100

101 **Table S1 X-ray Data collection and refinement statistics (related to Fig 1)**

	p110γ p84
<b>Data collection</b>	
Wavelength	0.9762
Space group	C121
Cell dimensions	
<i>a, b, c</i> (Å)	322.3, 166.6, 255.8
$\alpha, \beta, \gamma$ (°)	90, 114, 90
Resolution (Å)	90.3 - 8.5 (8.89-8.5)*
<i>R</i> <sub>merge</sub>	0.122 (0.39)
<i>I</i> / $\sigma I$	6.8 (4.4)
CC1/2	0.99 (0.90)
Completeness (%)	99.9%
Redundancy	5.8
<b>Refinement</b>	
Resolution (Å)	90.3 - 8.5 (8.89-8.5)
No. unique reflections	10833 (1084)
<i>R</i> <sub>work</sub> / <i>R</i> <sub>free</sub>	27.9/33.9
No. atoms	
Protein	50,008
<i>B</i> -factors	
Protein	545.9
Clash score	5.72
Ramachandran favored	98.29
Ramachandran outliers	0.07
Rotamer outliers	0.50
R.m.s. deviations	
Bond lengths (Å)	0.004
Bond angles (°)	0.64

102 \*Values in parentheses are for highest-resolution shell.

103 Number of crystals used for structure=1

104

105

106 **Table S2. HDX-MS data processing table (Related to Fig 2+4)**

	Figure 2D+E			Figure 2G			
Protein Data Set	p110γ apo	p110γ -p84	P110 γ -p101	p110γ -p84 high	p110γ -p84 low	p110γ -p101 high	p110γ -p101 low
HDX reaction details	%D <sub>2</sub> O= 91.7% pH(read)= 7.5 Temp= 18°C			%D <sub>2</sub> O= 47.2% pH(read)= 7.5 Temp= 18°C			
HDX time course	3s, 30s, 300s, 3000s at 18°C  3s at 4°C			30s, 300s			
HDX controls	N/A			N/A			
Back-exchange	No correction for back exchange, only correction was for %D <sub>2</sub> O			No correction for back exchange, only correction was for %D <sub>2</sub> O			
Number of peptides	166			173			
Sequence coverage	94.4			75.7			
Average peptide length / Redundancy	Length = 12.9 Redundancy = 1.9			Length = 10 Redundancy = 1.6			
Replicates	3	3	3	3 for 30s 2 for 300s	3 for 30s 2 for 300s	3 for 30s 2 for 300s	3 for 30s 2 for 300s
Repeatability Average SD =	0.6%	0.6%	0.6%	1.1%	1.6%	1.2%	1.0%
Significant differences in HDX	>5% and >0.4 Da and unpaired t-test <0.01			>7% and >0.5 Da and unpaired t-test <0.01			

107 SD = standard deviation from 3 technical replicates

108

109

110

111

112

113

114

115

116

117 **Table S2. HDX-MS data processing table (cont.)**

	Figure 4				
Protein Data Set	p110γ - p84 apo	p110γ-p84 memb	p110γ -p84 Ras+ memb	p110γ -p84 Gby+ memb	p110γ -p84 Gby+Ras + memb
HDX reaction details	%D <sub>2</sub> O= 65.5% pH(read)= 7.5 Temp= 18°C				
HDX time course	3s, 30s, 300s, 3000s				
HDX controls	N/A				
Back-exchange	Corrected based on %D <sub>2</sub> O				
Number of peptides	148 for p110γ, 100 for p84				
Sequence coverage	p110= 85.2 p85= 85.8				
Average peptide length / Redundancy	p110 Length = 13.1 p110 Redundancy = 1.8  p85 Length = 12.9 p85 Redundancy = 1.8				
Replicates	3	3	3	3	3
Repeatability Average SD	p110=0.6% p84 =0.7%	p110=0.7% p84= 0.9%	p110=0.7% P84=1%	p110=0.7% P84=0.9%	p110=0.7% P84=0.9%
Significant differences in HDX	>5% and >0.4 Da and unpaired t-test <0.01				

118

119 SD = standard deviation from 3 technical replicates

120

121

122

123

124

125

126

127

128 **TABLE S3. Single molecule TIRF microscopy parameters (related to Fig 5)**

129

DY647-PI3K visualized	input	$\tau_1 \pm SD$ (s)	$\tau_2 \pm SD$ (s)	$\alpha \pm SD$	<i>N</i>	$D_1 \pm SD$ ( $\mu\text{m}^2/\text{s}$ )	$D_2 \pm SD$ ( $\mu\text{m}^2/\text{s}$ )	$\alpha \pm SD$	steps
p84-p110 $\gamma$	Ras	0.041 $\pm$ 0.004	0.146 $\pm$ 0.05	0.81 $\pm$ 0.05	9741	0.215 $\pm$ 0.024	1.09 $\pm$ 0.028	0.23 $\pm$ 0.04	34896
p84-p110 $\gamma$	G $\beta$ $\gamma$	0.024 $\pm$ 0.001	—	—	11003	n.d.	n.d.	n.d.	n.d.
p84-p110 $\gamma$	Ras, G $\beta$ $\gamma$	0.042 $\pm$ 0.009	0.194 $\pm$ 0.01	0.10 $\pm$ 0.03	5134	0.045 $\pm$ 0.011	0.137 $\pm$ 0.021	0.36 $\pm$ 0.11	44104
p101-p110 $\gamma$	Ras	0.059 $\pm$ 0.003	0.324 $\pm$ 0.04	0.79 $\pm$ 0.04	6952	0.078 $\pm$ 0.06	0.640 $\pm$ 0.023	0.37 $\pm$ 0.04	19683
p101-p110 $\gamma$	G $\beta$ $\gamma$	0.399 $\pm$ 0.111	1.06 $\pm$ 0.31	0.53 $\pm$ 0.15	11414	0.095 $\pm$ 0.007	0.291 $\pm$ 0.042	0.59 $\pm$ 0.08	152632
p101-p110 $\gamma$	Ras, G $\beta$ $\gamma$	0.549 $\pm$ 0.069	7.83 $\pm$ 1.34	0.67 $\pm$ 0.08	2790	0.014 $\pm$ 0.005	0.039 $\pm$ 0.008	0.49 $\pm$ 0.04	86469

130

131 SD = standard deviation from 2-4 technical replicates

132 *N* = total number of molecules tracked in 2-4 technical replicates

133 steps = total number of particle displacements measured in 2-4 technical replicates

134 alpha ( $\alpha$ ) = fraction of molecules with characteristic dwell time ( $\tau_1$ ) or diffusion coefficient ( $D_1$ ).

135 membrane composition: 96% DOPC, 2% PI(4,5)P<sub>2</sub>, 2% MCC-PE. Ras = Ras(GTP)

136 n.d. = not determined

137

138

139

140

141

142

143

144

145

146

147

148

149

150

151

152

153



154 **Supplemental Alphafold models (related to Fig 6)**

155 The following PDB files from the highest ranked alphafold-multimer searches of the Gβγ interface of  
156 p110γ and p101 are attached (**details on model quality in Fig S6 and S7**)

157 1. p101\_CTD\_Gbg\_Alphafold\_Final\_model

158 2. p101\_Gbg\_Alphafold\_Final\_model

159 3. p110\_helical\_Gbg\_Alphafold\_Final\_model

160 4. p110\_dABD\_Gbg\_Alphafold\_Final\_model

161 Residues with pLDDT scores less than 50 have been removed.

162

163 **Supplemental references**

164 1. Jumper, J., Evans, R., Pritzel, A., Green, T., Figurnov, M., Ronneberger, O., Tunyasuvunakool, K.,  
165 Bates, R., Žídek, A., Potapenko, A., et al. (2021). Highly accurate protein structure prediction with  
166 AlphaFold. *Nature* 596, 583–589. 10.1038/s41586-021-03819-2.

167 2. Varadi, M., Anyango, S., Deshpande, M., Nair, S., Natassia, C., Yordanova, G., Yuan, D., Stroe, O.,  
168 Wood, G., Laydon, A., et al. (2022). AlphaFold Protein Structure Database: massively expanding the  
169 structural coverage of protein-sequence space with high-accuracy models. *Nucleic Acids Research* 50,  
170 D439–D444. 10.1093/nar/gkab1061.

171